

## **Effect of Operating Parameters on the Inhibition Efficacy of Decanethiol**

Z. Belarbi, F. Farel, D. Young, M. Singer, S. Nesic  
Institute for Corrosion and Multiphase Technology  
Department of Chemical and Biomolecular Engineering  
Ohio University  
342 West State Street  
Athens, OH 45701

### **ABSTRACT**

The overall objective of the present research is to investigate the effect of operating parameters on the inhibition efficacy of decanethiol in top of the line corrosion (TLC). The effect of water condensation rates, monoethylene glycol (MEG), H<sub>2</sub>S and hydrocarbon on inhibitor efficacy was evaluated. It was found that the presence of MEG, variation of gas temperatures and water condensation rates did not affect the inhibition efficacy of decanethiol. In sour environments, decanethiol was able to reduce localized corrosion of carbon steel and change the morphology of corrosion products on samples exposed to 30 ppm H<sub>2</sub>S. In the presence of condensable hydrocarbon (heptane), decanethiol lost its inhibition efficacy and showed very poor persistency. This was due to its low solubility in water.

**Keywords:** CO<sub>2</sub>/H<sub>2</sub>S corrosion, top-of-the-line corrosion, inhibition, decanethiol

## INTRODUCTION

Top-of-the-line corrosion (TLC) is recognized as one of the most serious concerns encountered in the pipeline transmission of hydrocarbons, where carbon steel is the principal tubular alloy of choice.<sup>1</sup> TLC occurs in wet gas transportation where temperature gradients between the internal surfaces of the pipeline and the outside environment leads to condensation of water, as well as lighter hydrocarbons from the gas phase. Corrosive gases dissolve into the condensed water formed on the upper surface of the pipe resulting in TLC. Extensive prior research has primarily focused on the use of volatile corrosion inhibitors (VCIs) to mitigate TLC.<sup>2,3,4</sup> The importance and relevance of VCIs are evidenced by the existence of several patents, as well as recent publication of comprehensive reviews thereof.<sup>5,6</sup> A few volatile organic compounds have been identified and tested as potential VCIs in the laboratory; their molecules have either filming or neutralizing properties.<sup>7,8</sup> The two different classes of volatile corrosion inhibitors examined in this research possessed amine or thiol functionalities. Based on the previously reported results, morpholine and diethylamine show poor inhibition properties; these amines solely increase the pH of the condensed water and do not significantly decrease the corrosion rate.<sup>7</sup> In contrast, thiols, especially decanethiol and 11-mercaptoundecanoic acid, show good persistency (in the absence of condensable hydrocarbons), filming behavior and superior mitigation of TLC.<sup>8</sup> The good persistency of decanethiol and 11-mercaptoundecanoic acid could be due to their low association by hydrogen bonding and their lower solubility in water.

The overall objective of the present research was to investigate the effect of different operating parameters on the inhibition efficacy of decanethiol. The effect of water condensation rate, monoethylene glycol (MEG), hydrogen sulfide (H<sub>2</sub>S) and hydrocarbon on inhibitor efficacy was evaluated.

The presence of hydrocarbons can affect TLC either by changing the water wetting of the steel surface or by influencing the water chemistry of the system. Pojtanabuntoeng, *et al.*,<sup>9</sup> investigated the influence of hydrocarbon co-condensation (*n*-heptane) on top of the line corrosion. In a hydrocarbon-free system, condensed water wetted the entire specimen surface and the TLC rate increased with the water condensation rate. However, the presence of *n*-heptane, which condensed at a rate seven times faster than water, led to segregation of water droplets and oil-wetting on most of the sample surface. Changes in the water droplet chemistry caused a rapid formation of iron carbonate on the steel surface. While corrosion was low on oil-wetted parts, the TLC rates underneath condensed water droplet remained relatively high.

Monoethylene glycol (MEG) is a common chemical added to wet gas pipelines to prevent the formation of gas clathrates (hydrates).<sup>10</sup> A mechanistic model was developed to predict the MEG concentration in the condensing phase, and the condensation rate of water and MEG at the top of a wet gas pipeline.<sup>11</sup> For this purpose, it is important to investigate the effect of MEG on the inhibition efficacy of decanethiol.

## EXPERIMENTAL PROCEDURE

### Materials and Chemicals

Specimens used for weight loss experiments and surface analysis were made of API<sup>(1)</sup> 5L X65 carbon steel with a tempered martensitic microstructure; its chemical composition is given in Table 1. Decanethiol and heptane used in this research were acquired from Sigma-Aldrich<sup>(2)</sup>.

---

<sup>(1)</sup> American Petroleum Institute (API), 1220 L St. NW, Washington, DC 20005.

<sup>(2)</sup> Trade name

Table 1  
Composition (wt.%) of the API<sup>(1)</sup> 5L X65 carbon steel used in this research

| Element | C    | Nb   | Mn   | P     | S      | Ti   | V    | Ni   | Fe      |
|---------|------|------|------|-------|--------|------|------|------|---------|
| X65     | 0.05 | 0.03 | 1.51 | 0.004 | <0.001 | 0.01 | 0.04 | 0.04 | balance |

## Experimental Procedure

The experimental setup used for evaluating the effect of water condensation rate (WCR), monoethylene glycol (MEG), H<sub>2</sub>S and hydrocarbon on the inhibition efficacy of decanethiol is shown in Figure 1. Weight loss specimens were used to measure the corrosion rate at the top-of-the-line. The bulk aqueous phase comprised of a 1 wt.% NaCl electrolyte, sparged with CO<sub>2</sub> for 2 hours to facilitate deoxygenation and ensure saturation in acid gas. API 5L X65 carbon steel samples (exposed area = 7.92 cm<sup>2</sup>) were polished using silicon carbide abrasive paper (600 grit), cleaned with isopropanol in an ultrasonic bath, and dried at room temperature before their introduction into the glass cell. Two weight loss specimens were flush-mounted at the top of the experimental setup, which was equipped with a cooling system to control its temperature. The corrosion rate of the specimen at the top (TLC rate) was measured following the ASTM<sup>(3)</sup> G1 standard.<sup>12</sup> The detailed experimental matrix to study the effect of WCR on inhibition efficacy of decanethiol is shown in Table 2.

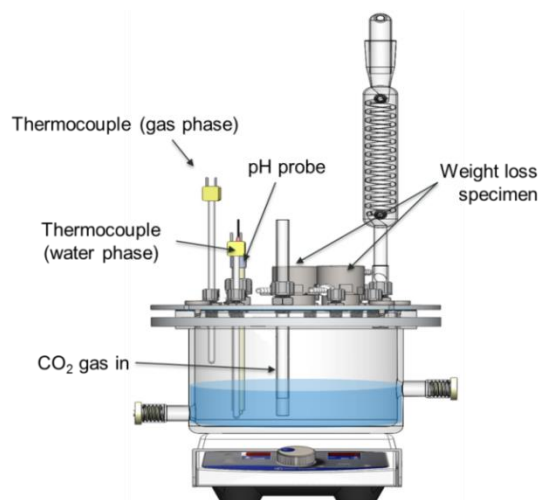


Figure 1: Experimental setup for evaluating efficacy of VCI candidates for TLC.

Table 2  
Experimental matrix to study the effect of WCR on inhibition efficacy of decanethiol

|   |             |      |     |     |
|---|-------------|------|-----|-----|
| Gas temperature (°C)                        | 40          | 65   | 87  |     |
| Steel temperature (°C)                      | 30          | 30   | 67  | 30  |
| Total pressure (bar)                        | 1           |      |     |     |
| Solution                                    | 1 wt.% NaCl |      |     |     |
| pH bottom solution                          | 4           |      |     |     |
| Inhibitor concentration at the bottom (ppm) | 400         |      |     |     |
| Calculated WCR (mL/m <sup>2</sup> /s)       | 0.12        | 0.56 | 0.9 | 2.2 |
| Test duration (days)                        | 3           |      |     |     |

<sup>(3)</sup> American Society for Testing and Materials (ASTM), 100 Barr Harbor Drive, West Conshohocken, PA, 19428-2959.

The study of the effect of H<sub>2</sub>S on inhibition efficacy of VCIs was done under the test conditions shown in Table 3., in the same glass cell presented in Figure 1, Prior to each experiment, the bottom solution was deoxygenated for 2 hours. Then, H<sub>2</sub>S and CO<sub>2</sub> were mixed with the aid of a rotameter to achieve the desired concentration of H<sub>2</sub>S. This gas mixture was continuously purged into the glass cell throughout the experiment duration. The effluent gas was neutralized with activated carbon.

Table 3  
Experimental matrix to study the effect of H<sub>2</sub>S on inhibition efficacy of decanethiol as a VCI

|   |          |
|---|----------|
| Gas temperature (°C)                        | 40       |
| Steel temperature (°C)                      | 38       |
| Total pressure (bar)                        | 1        |
| Solution                                    | DI water |
| pH bottom solution                          | 4        |
| Inhibitor concentration at the bottom (ppm) | 0, 400   |
| Calculated WCR (mL/m <sup>2</sup> /s)       | 0.005    |
| Test duration (days)                        | 3, 7     |
| H <sub>2</sub> S concentration (ppm)        | 30       |

In the presence of heptane, the performance of decanethiol was evaluated first under bottom-of-the line (BLC), then under TLC conditions. This enabled comparison and validation of inhibition mechanism for the two scenarios: under constant water immersion and under condensing water conditions. A concentration of 400 ppm<sub>v</sub> of decanethiol was added into the deoxygenated 1 wt.% NaCl (1.2 L) / heptane (0.6L) mixture and then the BLC and TLC corrosion rates were measured for 14 hours and 3 days, respectively. For BLC tests, an electrochemical cell with a three-electrode configuration was used. A carbon steel API X65 rotating cylinder electrode (RCE), a platinum grid, and an Ag/AgCl<sub>(saturated)</sub> electrode were used as working, counter, and reference electrodes, respectively. The setup and procedure for testing in BLC conditions are based on those used by Belarbi, *et al.*<sup>7</sup> For TLC tests, the weight loss method was used to measure corrosion rate. Another series of tests was performed to better understand the mechanisms of inhibition of decanethiol in the presence of heptane. Deoxygenated heptane (0.6 L) was added after 4 hours of exposure for BLC test and after 2 days of exposure for TLC test. This way, the thiols would have already adsorbed on the steel surface and the persistency of the film could be evaluated. Although it is recognized that this procedure does not relate to any specific production scenario, it was thought that it could nevertheless yield interesting information about the inhibition mechanism.

## Surface Analysis

Surface analysis of the exposed specimens was performed with a JEOL JSM-6090 LV scanning electron microscope (SEM) and an EDAX energy dispersive X-ray spectroscopy (EDS) system. Imaging was performed at an accelerating voltage of 15 kV using a secondary electron detector (SEI).

## RESULTS AND DISCUSSION

### Effect of water condensation rate on inhibition efficacy of decanethiol

The inhibitor efficacy at the top-of-the-line was evaluated at different condensation rates. Comparisons of TLC rates with and without inhibitor for top-of-the-line samples are shown in Figure 2. In the absence of decanethiol, the results show that the increase of condensation rates increases

corrosion rates of carbon steel (Figure 2.a). Many papers<sup>1,13</sup> have been published describing the main effect of gas bulk and pipe wall temperature and condensation rates on TLC in CO<sub>2</sub> dominated environments. These parameters influence the corrosion rate in a complicated way, however a common behavior is generally observed. At low condensation rate, the accumulation of ferrous ions in the condensed water will increase the pH, resulting in the formation of a protective FeCO<sub>3</sub> corrosion product layer. At high condensation rates, the dissolved iron is continuously flushed away. This leads to a lower condensed water pH and instability of iron carbonate, resulting in higher TLC rate.<sup>14</sup>

In the present tests series, general corrosion attack was observed on the surface of samples at condensation rates of 0.12, 0.56 and 2.2 mL/m<sup>2</sup>/s. Due to the low surface temperature, the slow kinetics of FeCO<sub>3</sub> formation prevented its precipitation within the timeframe of the experiment. Instead, only Fe<sub>3</sub>C corrosion product residues were detected on the specimen surface (Figure 3, Figure 4 and Figure 6). However, at condensation rates of 0.9 ml/m<sup>2</sup>/s (Figure 2.b) and at a gas temperature of 87°C, a protective layer of iron carbonate formed on the surface, which lowered the corrosion rate (Figure 5). The formation of this layer is governed by the FeCO<sub>3</sub> saturation level in the condensed liquid film and the precipitation kinetics of the corrosion product. In the presence of decanethiol and at all condensation rates tested, the specimen surface was fully protected (CR ≤ 0.06 mm y<sup>-1</sup>) and no corrosion product was observed on the steel surface after 2 days of exposure (Figure 2). Decanethiol provided inhibition efficacy higher than 87%. SEM images (Figure 3, Figure 4, Figure 5 and Figure 6) showed mechanical polishing lines marks on the substrate surface and no corrosion product was detected. This means that decanethiol was able to protect the steel samples exposed to top-of-the-line conditions in all gas temperatures and water condensation rates tested. This shows that the inhibitor efficacy was not affected by the condensation rate.

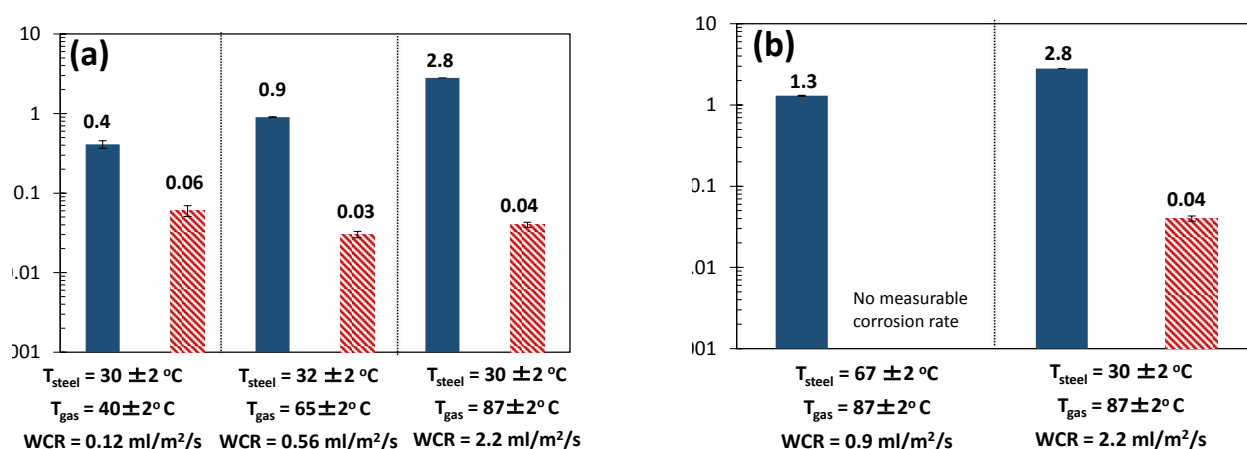


Figure 2: Corrosion rate by weight loss measurement of the uninhibited (■) and inhibited (▨) TLC specimens at different water condensation rates (WCR) after 2 days.a): effect of gas temperature. b): effect of specimen temperature.

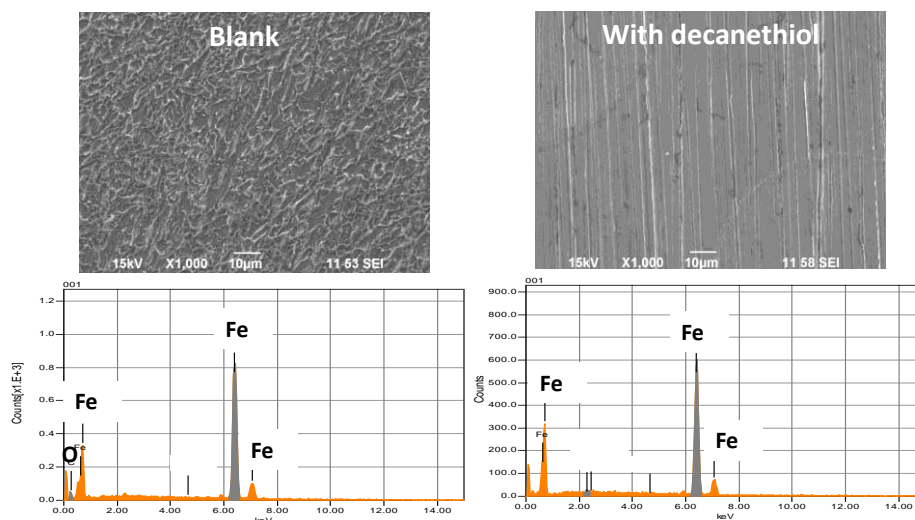


Figure 3: SEM and EDS surface analysis of X65 carbon steel with and without corrosion inhibitor,  
 $T_{\text{gas}} = 40 \pm 2 \text{ }^{\circ}\text{C}$ ,  $T_{\text{specimen}} = 30 \pm 2 \text{ }^{\circ}\text{C}$ ,  $\text{WCR} = 0.12 \text{ mL/m}^2/\text{s}$ .

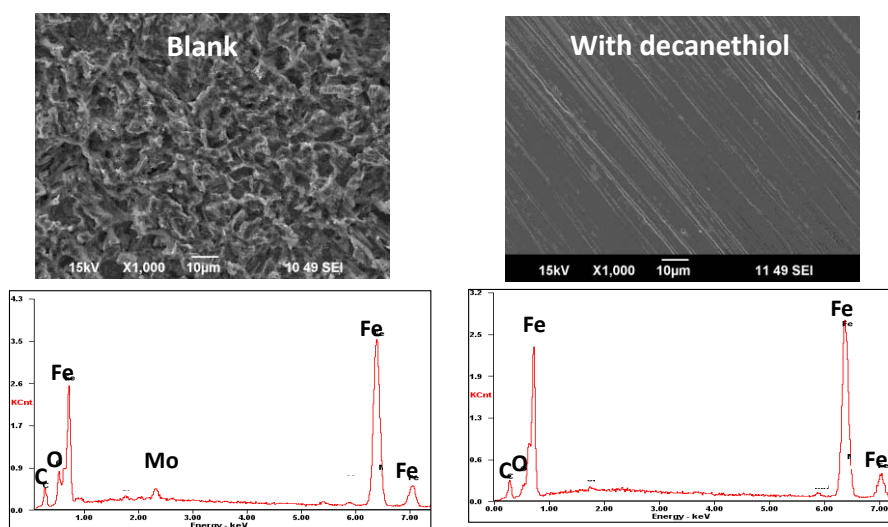


Figure 4: SEM and EDS surface analysis of X65 carbon steel with and without corrosion inhibitor,  
 $T_{\text{gas}} = 65 \pm 2 \text{ }^{\circ}\text{C}$ ,  $T_{\text{specimen}} = 32 \pm 2 \text{ }^{\circ}\text{C}$ ,  $\text{WCR} = 0.56 \text{ mL/m}^2/\text{s}$ .

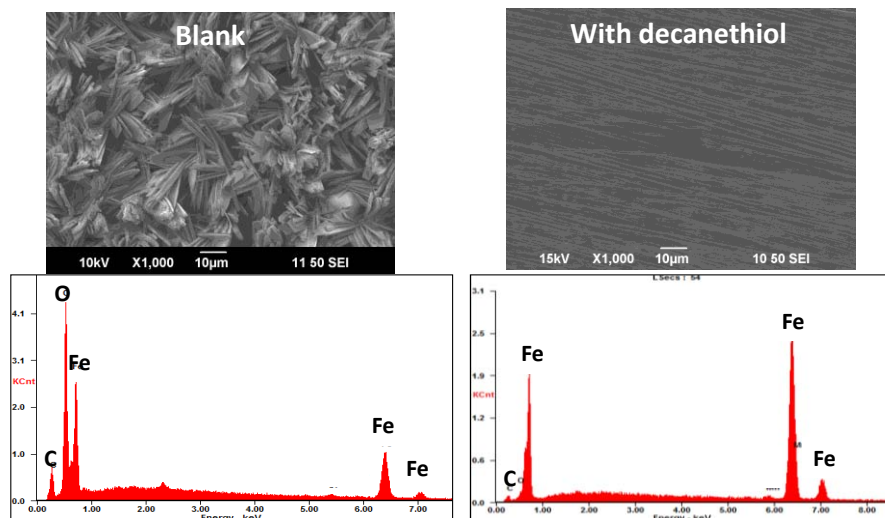


Figure 5: SEM and EDS surface analysis of X65 carbon steel with and without corrosion inhibitor,  $T_{\text{gas}} = 87 \pm 2 \text{ }^{\circ}\text{C}$ ,  $T_{\text{specimen}} = 67 \pm 2 \text{ }^{\circ}\text{C}$ ,  $\text{WCR} = 0.9 \text{ mL/m}^2/\text{s}$ .

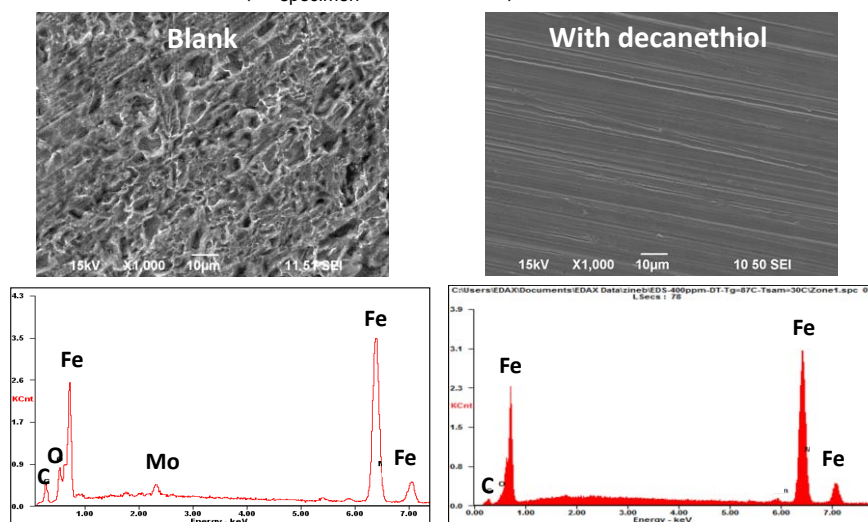


Figure 6: SEM and EDS surface analysis of X65 carbon steel with and without corrosion inhibitor,  $T_{\text{gas}} = 87 \pm 2 \text{ }^{\circ}\text{C}$ ,  $T_{\text{specimen}} = 30 \pm 2 \text{ }^{\circ}\text{C}$ ,  $\text{WCR} = 2.2 \text{ mL/m}^2/\text{s}$ .

### Effect of monoethylene glycol on inhibition efficacy of decanethiol

Figure 7 shows the corrosion rate that was measured from weight loss specimens at the top-of-the-line in the presence of monoethylene glycol (MEG). Considering 50 wt. % MEG in the bulk liquid phase, the average TLC rate was almost the same as in MEG free conditions. This can be explained by the facts that MEG does not readily evaporate and condense at the top of the line and that 50 wt.% MEG has no visible effect on condensation rate. SEM images and associated EDS spectra (not shown in this paper) typically show the same iron carbonate layer formed in MEG free environments. In the presence of decanethiol, un-inhibited and inhibited TLC rates were also the same (around  $0.04 \text{ mm.y}^{-1}$ ). The surface of the X65 specimen was fully protected as the SEM (Figure 8) micrographs show polishing lines on the substrate surface and EDS analysis shows a presence of sulfur peak which could be due to adsorption of decanethiol.



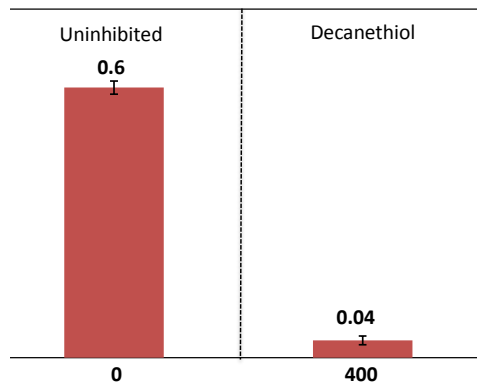


Figure 7: Corrosion rate by weight loss measurement of the uninhibited and inhibited TLC specimens (WCR = 0.55 mL/m<sup>2</sup>/s). 50 wt.% MEG.

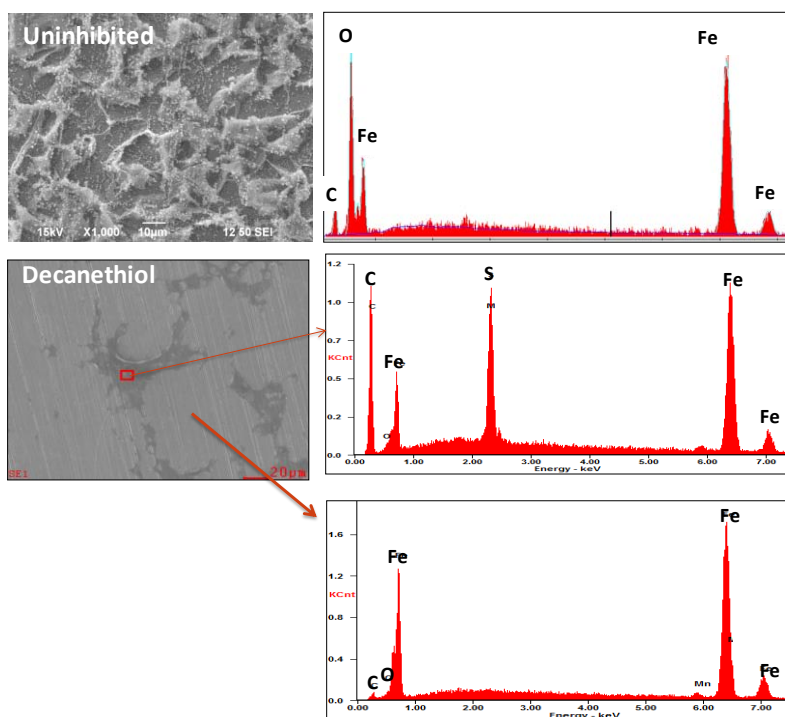


Figure 8: SEM images and EDS analysis of sample exposed to corrosion in the co-condensation of water and 50 wt.% MEG (WCR = 0.55 mL/m<sup>2</sup>/s).

### Effect of H<sub>2</sub>S on inhibition efficacy of decanethiol

TLC results from weight loss analysis with and without decanethiol in the presence of 30 ppm H<sub>2</sub>S are shown in Figure 9. The presence of traces of H<sub>2</sub>S in CO<sub>2</sub> environments retards the general TLC rate through formation of an iron sulfide layer. In a mixed CO<sub>2</sub>/H<sub>2</sub>S environment, iron sulfide often dominates the layer composition regardless of the value of CO<sub>2</sub> partial pressure. This explains the reduction of corrosion rate in the presence of H<sub>2</sub>S as iron sulfide is formed, conferring some protection to the steel surface. These results are in good agreement with the literature.<sup>15,16</sup> In the presence of decanethiol, TLC corrosion rate decreased from 0.1 mm y<sup>-1</sup> to 0.05 mm y<sup>-1</sup> after 3 days. In sour systems, decanethiol provides 50% of inhibition efficacy. However, this result should be taken cautiously considering the already low value of the un-inhibited TLC rate. Representative SEM images, which show the morphology of the FeS layer attached to the steel surface with and without



decanethiol, are displayed in Figure 10. Generally, the FeS layer consists of two distinct layers attached to the steel. A two-step mechanism involving the rapid initial formation of a thin FeS layer, identified as mackinawite, on the metal surface which can be overlain by different phases of iron sulfide has been described by Smith.<sup>17</sup> However, in the presence of decanethiol, the morphology of corrosion product changed (Figure 10). Experimental time was extended from 3 to 7 day, following the experimental procedure described previously, to confirm the effect of decanethiol on mitigation of sour TLC and investigate the occurrence of localized corrosion. Overall, no significant difference in general corrosion rate and corrosion product morphology was observed between 3 days and 7 days exposure time (Figure 9). The average general corrosion rate was between 0.04 and 0.07 mm y<sup>-1</sup>. On the other hand, the presence of 30 ppm H<sub>2</sub>S during 7 days of experiment resulted in a pit penetration rate 1.34 mm y<sup>-1</sup> (Figure 11). The pit penetration rate was calculated from the depth of the deepest pit measured by profilometry analysis (25.7 μm). This behavior is due to competition between HS<sup>-</sup> (formed from H<sub>2</sub>S) and thiol to absorb on the steel surface.

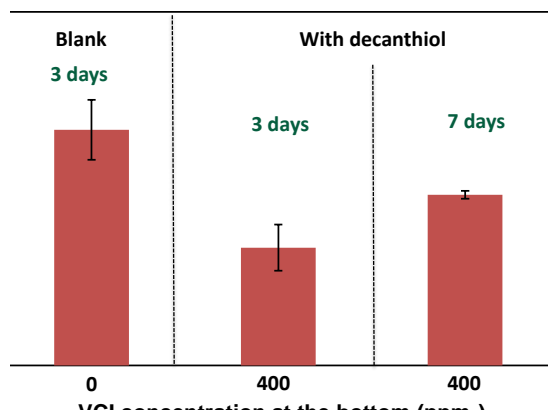


Figure 9: Weight loss TLC rate in presence of 30 ppm H<sub>2</sub>S with and without decanethiol at the bottom. T<sub>gas</sub> = 40 °C, T<sub>specimen</sub> = 38 °C, WCR = 0.005 mL/m<sup>2</sup>/s.

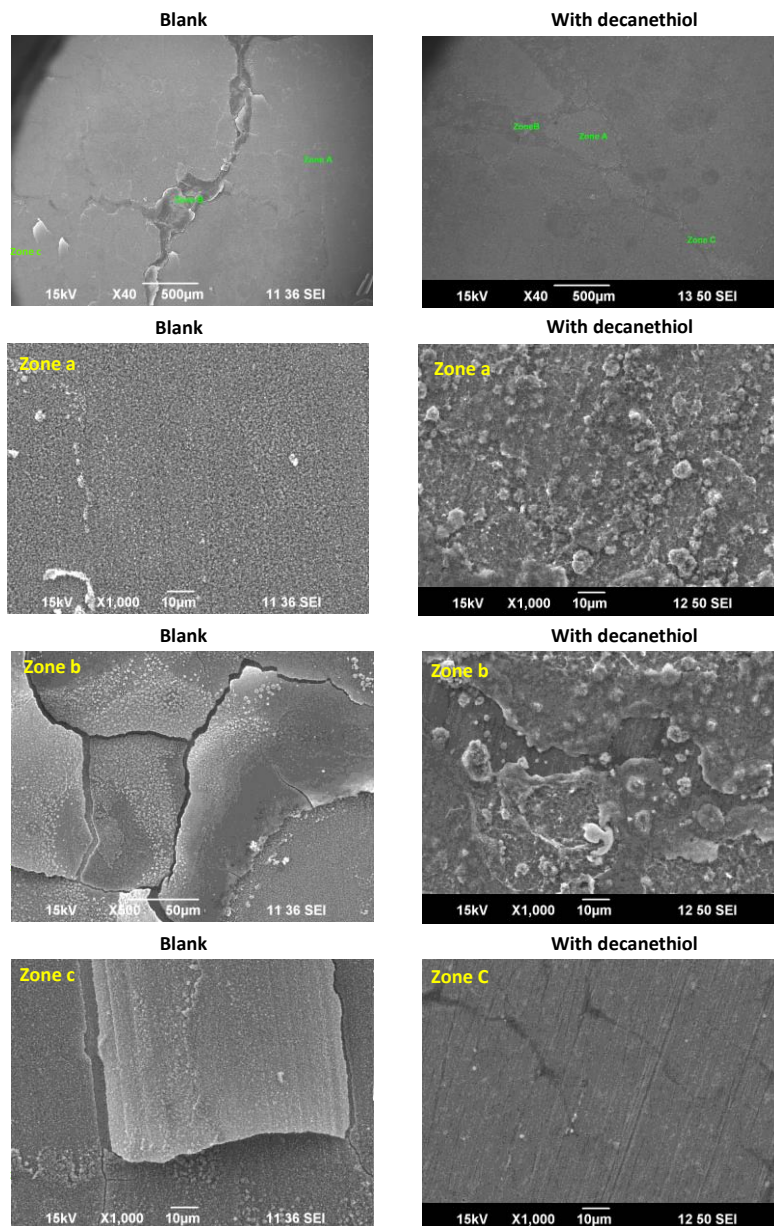


Figure 10: SEM surface analysis in the presence of 30 ppm  $H_2S$  with and without inhibitor after 3 days of exposure.

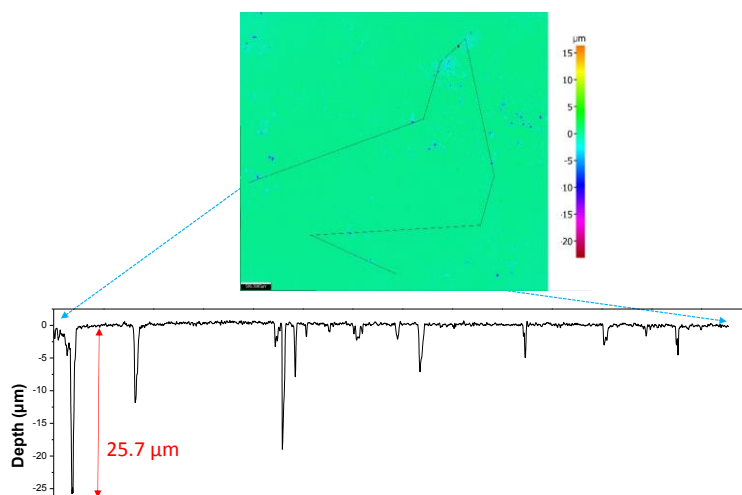


Figure 11: Surface topography after removal of the corrosion product.

## Identification of residence time of decanethiol in presence of hydrocarbon

### Bottom-of-the-line

A concentration of 400 ppm<sub>v</sub> of decanethiol was added into the solution/heptane mixture and the corrosion rate and OCP were then measured for approximately 14 hours. The results are presented in Figure 12. The corrosion rate and OCP in the presence and absence of decanethiol were similar. It is possible that all the decanethiol in the water phase diffused to the oil phase (heptane) due to its higher solubility in heptane. A similar behavior was observed when the steel sample was immersed in heptane/inhibitor for 1 hour, and then returned to the water phase for 14 hours. A possible explanation is that the affinity between inhibitor/steel is lower than the affinity between inhibitor/heptane, preventing adsorption of inhibitor on the steel surface.

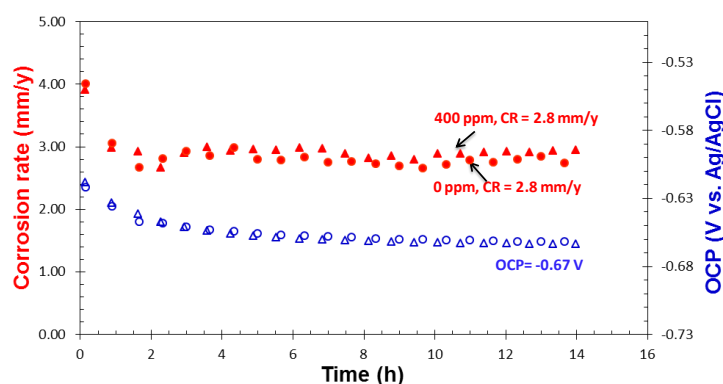


Figure 12: OCP and BLC rate of X65 rotating cylinder electrode in 1 wt.% NaCl solution at 25°C as a function of time. The red points are the BLC rates (●: 0 ppm<sub>v</sub>, ▲: 400 ppm<sub>v</sub>), and the blue points are OCP (○: 0 ppm<sub>v</sub>, △: 400 ppm<sub>v</sub>).

The performance of decanethiol was further evaluated in the presence of heptane by another procedure; the BLC rates was measured for 4 hours in 1.2 L of 1 wt.% NaCl in the presence of 400 ppm<sub>v</sub> of decanethiol. After that, 0.6 L of deoxygenated heptane was added, making sure that the corrosion specimen remained immersed in the aqueous phase. The results are shown in Figure 13.

During this time the corrosion rate did not change significantly (from 0.02 to 0.03 mm y<sup>-1</sup>), meaning that decanethiol was still adsorbed on the surface and the adsorption of decanethiol on the steel surface was strong. The SEM analysis (Figure 14) still shows the polishing lines on the substrate surface. It is important to mention that the presence of sulfur was detected via EDS analysis (no sulfur was found in the absence of heptane).

The performance of the decanethiol was further evaluated in the presence of heptane by another procedure; corrosion rate was measured for 4 hours in 1.2 L of 1 wt.% NaCl in the presence of 400 ppmv of decanethiol. After that, 0.6 L of deoxygenated heptane was added. The steel specimen was moved into the oil phase for 1 hour and then returned to the water phase. Corrosion rate and OCP was monitored during 25 more hours (not shown in this paper). Corrosion rate and OCP did not significantly change, which implies a strong adsorption of decanethiol on the steel surface.

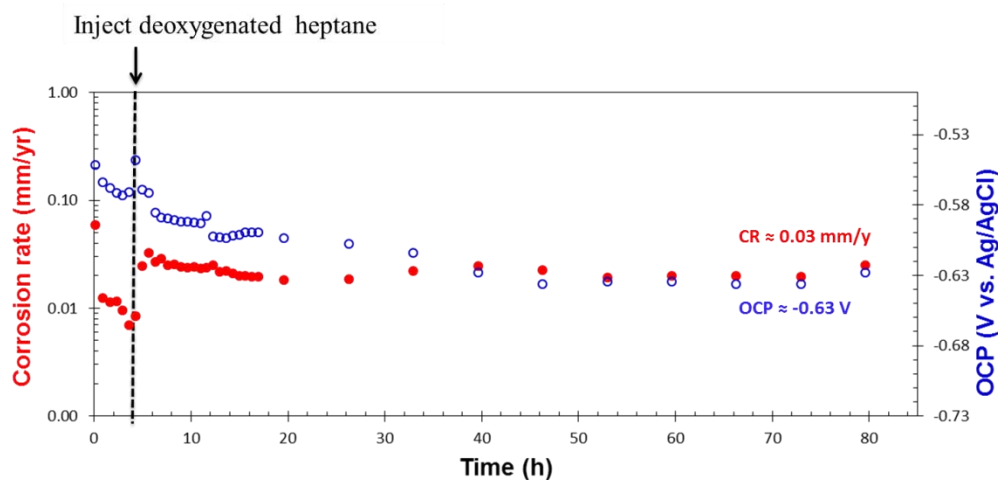


Figure 13: OCP and BLC rate of X65 rotating cylinder electrode in 1 wt.% NaCl solution at 25°C as a function of time. The red points are the BLC rates, and the blue points are OCP.

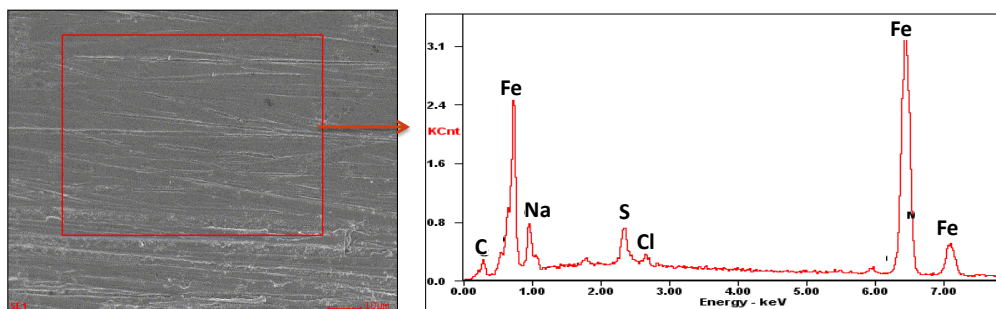


Figure 14: SEM images and EDS analysis of the sample surfaces after the inhibition tests with 400 ppm<sub>v</sub> of inhibitor after 80 h of immersion.

### Top-of-the-line

Weight loss results concerning the efficacy of VCIs at the top-of-the-line are shown in Figure 15. The corrosion rates in the presence and absence of decanethiol are similar showing poor inhibition efficacy. It is possible that all the inhibitor present in the mixture diffused to the oil phase (heptane), because of the partition of VCIs between water and heptane. No protective layer could form when the

sample was exposed to n-heptane/water co-condensing environment. The specimen surface for the tests with and without inhibitor and in the presence of heptane lost its mirror finish indicating active corrosion. One possible explanation is the interaction between inhibitor tails and heptane molecules. The inhibitor/steel affinity is lower than for inhibitor/heptane, also preventing adsorption of inhibitor. Figure 16 show the SEM images and EDS analysis of the sample exposed to co-condensation of water and n-heptane before the removal of corrosion products. Iron carbonate was observed in the presence and the absence of decanethiol. The SEM analysis performed after removal of the corrosion product layer did not show signs of localized corrosion.

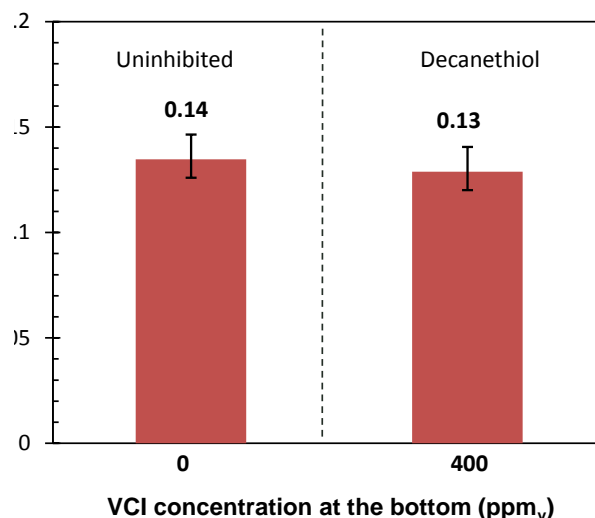


Figure 15: Corrosion rate by weight loss measurement of the uninhibited and inhibited TLC specimens (WCR = 0.2 mL/m<sup>2</sup>/s, HCR = 1.4 mL/m<sup>2</sup>/s).

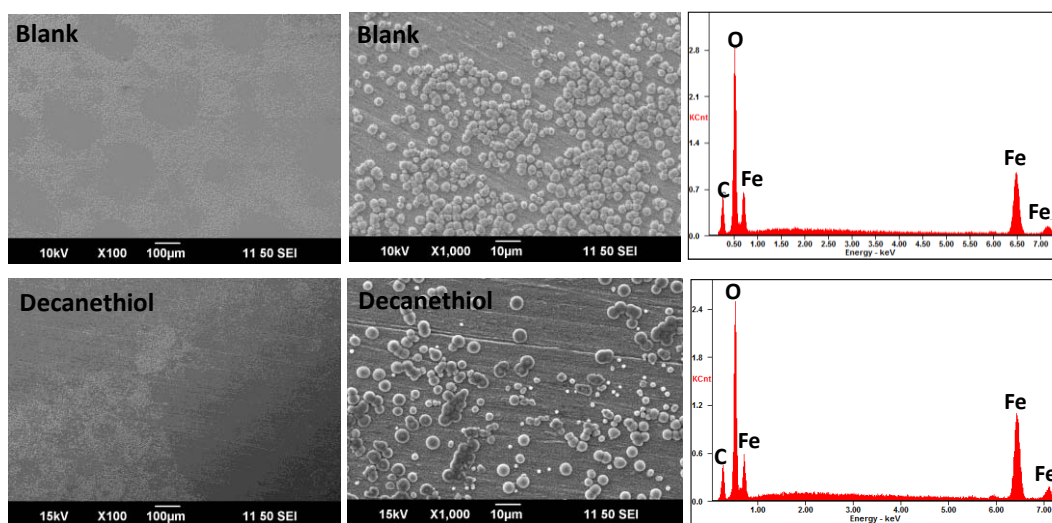


Figure 16: SEM/EDS analysis of sample exposed to corrosion in the co-condensation of water and heptane (WCR = 0.2 mL/m<sup>2</sup>/s, HCR = 1.4 mL/m<sup>2</sup>/s) in the presence and absence of decanethiol.

Another series of tests was performed to better understand the mechanisms of inhibition of decanethiol in the presence of heptane. TLC rates were measured after 2 days of exposure in 1.2 L of 1wt.% NaCl in the presence of decanethiol. The test was then repeated but 0.6 L of deoxygenated



heptane was added to the cell after 2 days of exposure time and TLC rates were monitored over two additional days. During the first two days of exposure (without heptane), decanethiol showed excellent inhibition efficacy. After adding heptane, it is evident that the steel surface started to corrode as it lost its characteristic shine (Figure 17). Weight loss data (Figure 18) showed that the corrosion rates measured for the entire 4 days of exposure time were twice as high compared to the environment without heptane. This indicates that the thiols present in the water phase diffused to the condensing oil phase (heptane) because of its high solubility in heptane, leading to a loss of persistency. One plausible explanation involves the interaction between inhibitor tails and heptane molecules. The affinity inhibitor/steel is lower than the affinity inhibitor/heptane, favoring desorption of the inhibitor. Figure 19 shows SEM micrographs and EDS analysis of the sample exposed to co-condensation of water and n-heptane before the removal of corrosion products. As can be noticed, some crystals of iron carbonate were observed as signs of active corrosion and water droplet segregation.

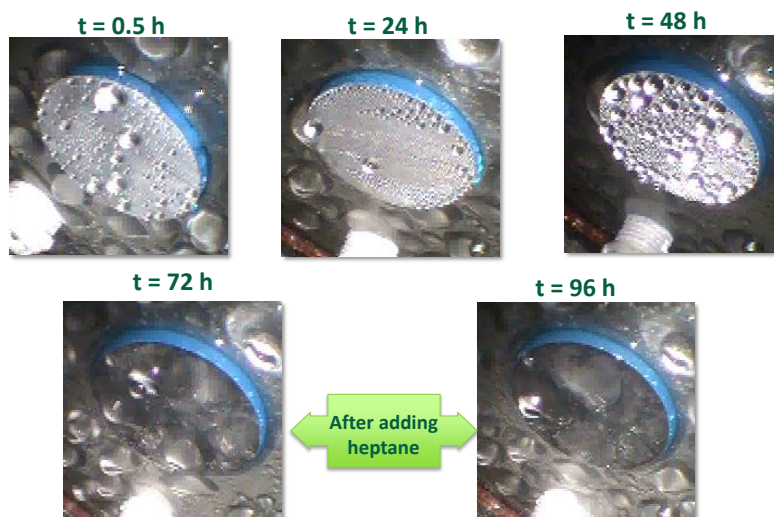


Figure 17: Samples exposed to corrosion with co-condensation of water with decanethiol.

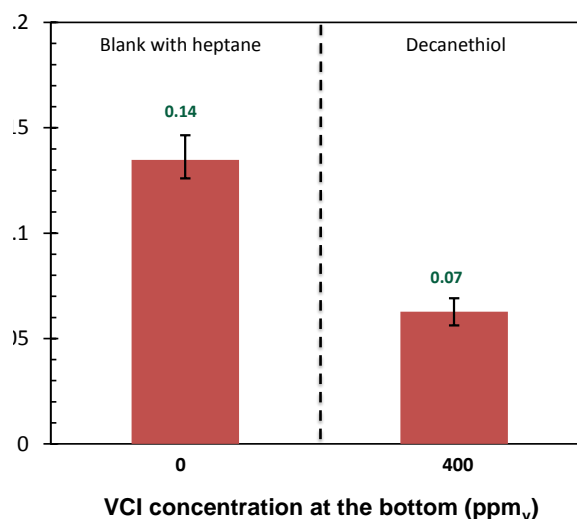


Figure 18: Corrosion rate by weight loss measurement of the uninhibited and inhibited TLC specimens (WCR = 0.2 mL/m<sup>2</sup>/s, HCR = 1.4 mL/m<sup>2</sup>/s).

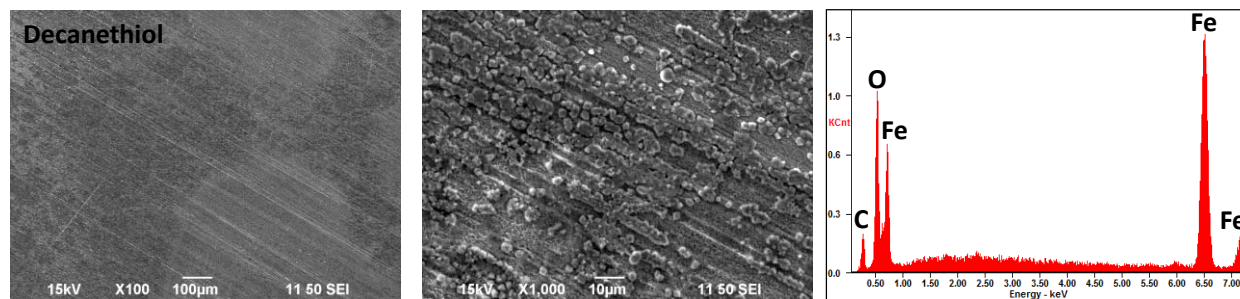


Figure 19: SEM images and EDS analysis of sample exposed to corrosion in the co-condensation of water and heptane ( $WCR = 0.2 \text{ mL/m}^2/\text{s}$ ,  $HCR = 1.4 \text{ mL/m}^2/\text{s}$ ) in the presence of inhibitor after 4 days.

## CONCLUSIONS

The following results can be drawn from this study:

- Decanethiol was able to protect the steel samples exposed to top-of-the-line conditions at all gas temperatures and water condensation rates tested.
- The presence of 50 wt% MEG in the bulk aqueous phase did not affect inhibition efficiency of decanethiol.
- Decanethiol was able to reduce localized corrosion of carbon steel and change the morphology of corrosion product on samples exposed to 30 ppm  $\text{H}_2\text{S}$ .
- In the presence of a non-polar solvent (heptane), no adsorption of thiols happened on the steel surface leading to poor inhibition properties at the top of the line.
- Decanethiol lost its inhibition efficacy in the presence of heptane.
- Low residence time of decanethiol on the steel surface was observed in the presence of heptane.

## ACKNOWLEDGMENTS

The authors would like to thank the following companies for their financial support: Quadrant Energy, BHP Billiton, BP, Chevron, ConocoPhillips, MI-Swaco, Petronas, PTTEP, Woodside and Repsol. Also, the technical support from the lab's staff at Institute for corrosion and multiphase technology by Mr. Alexis Barxias and Mr. Cody Shafer is highly appreciated.

## BIBLIOGRAPHY

1. Y. Gunaltun and D. Larrey, "Correlation of cases of top of line corrosion with calculated water condensation rates," in *CORROSION/2000, Paper no. 71*, Houston, TX: NACE 2000.
2. Y. Gunaltun, T. E. Pou, M. Singer, C. Duret and S. Espitalier, "Laboratory testing of volatile corrosion inhibitors," in *CORROSION/2010, Paper no. 10095*, Houston, TX: NACE 2010.
3. S. Punpruk, M. Thammachart and Y. Gunaltun, "Field testing of volatile corrosion inhibitors and batch treatment efficiency by cooled probe," in *CORROSION/2010 - paper no. 14334*, Houston, TX: NACE 2010.
4. Y. Gunaltun and L. Payne, "A new technique for the control of top of line corrosion : TLCC-PIG," in *CORROSION/2003 - paper no. 03344*, Houston, TX: NACE 2003.
5. R. Inzunza, B. Valdez and M. Schorr, "Corrosion inhibitor patents in industrial applications – A review," *Recent Patents on Corrosion Science*, vol. 3, pp. 71-78, 2013.



6. V. Saji, "A review on recent patents in corrosion inhibitors," *Recent Patents on Corrosion Science*, vol. 2, pp. 6-12, 2010.
7. Z. Belarbi, F. Farelas, M. Singer and S. Nesic, "Role of amines in the mitigation of CO<sub>2</sub> Top of the Line Corrosion," *Corrosion*, vol. 72, no. 10, pp. 1300-1310, 2016.
8. Z. Belarbi, T. N. Vu, F. Farelas, M. Singer and S. Nesic, "Thiols as volatile corrosion inhibitors for top of the line corrosion," *Corrosion*, vol. 73, no. 7, pp. 892-899, 2017.
9. T. Pojtanabuntoeng, M. Singer and S. Nesic, "Water/hydrocarbon co-condensation and the influence on top-of-the -line corrosion," in *CORROSION//2011 - paper no.11330*, Houston, TX: NACE 2011.
10. G. E.I. and J. Morard, "Why does glycol inhibit CO<sub>2</sub> corrosion?," in *CORROSION//1998 - paper no.221*, Houston, TX: NACE 1998.
11. S. Gue, F. Farelas and M. Singer, "A glycol/water co-condensation model to investigate the influence of monoethylene glycol on top-of-the-line corrosion," *Corrosion*, vol. 73, no. 6, pp. 742-755, 2017.
12. "Standard practice for preparing cleaning and evaluating corrosion test specimens," *ASTM-G1*, pp. 15-21, 1999.
13. S. Olsen and A. Dugstad, "Corrosion under dewing conditions," in *CORROSION//1993 - paper no.69*, Houston, TX: NACE 1993.
14. D. V. Pugh, S. L. Asher, J. Cai and W. J. Sisak, "Top-of-line corrosion mechanism for sour wet gas pipelines," in *CORROSION/2009, Paper no. 09285*, Houston, TX: NACE 2009.
15. A. Camacho, M. Singer, B. Brown and S. Nesic, "Top of the Line corrosion in H<sub>2</sub>S/CO<sub>2</sub> environments," in *CORROSION/2008, Paper no. 08470*, Houston, TX: NACE 2008.
16. N. Yaakob, M. Singer and D. Young, "Top of the line corrosion behavior in highly sour environments: effect of the gas/steel temperature," in *CORROSION/2014, Paper no. 3807*, Houston, TX: NACE 2014.
17. S. N. Smith, B. Brown and W. Sun, "Corrosion at higher concentrations and moderate temperature," in *CORROSION/2011, Paper no. 11081*, Houston, TX: NACE 2011.